Technical Report Documentation Page

1. Report No.	2. Government Accession No.	3. Recipient's Catalog No.
SWUTC/15/600451-00024-1		

4. Title and Subtitle	5. Report Date
ARTERIAL SIGNAL COORDINATION WITH UNEVEN DOUBLE CYCLING	January 2014
	6. Performing Organization Code

7. Author(s)	8. Performing Organization Report No.
Hongmin Zhou and H. Gene Hawkins, Jr.	

9. Performing Organization Name and Address	10. Work Unit No. (TRAIS)
Texas A&M Transportation Institute Texas A&M University System College Station, Texas 77843-3135	11. Contract or Grant No. DTRT12-G-UTC06

12. Sponsoring Agency Name and Address	13. Type of Report and Period Covered
Southwest Region University Transportation Center Texas A&M Transportation Institute Texas A&M University System College Station, Texas 77843-3135	14. Sponsoring Agency Code

15. Supplementary Notes

Supported by a grant from the U.S. Department of Transportation, University Transportation Centers Program.

16. Abstract

In arterial coordination, high traffic volume at large intersections often requires a long cycle length to achieve good two-way progression. This long cycle length, however, often causes excessive delay at some minor intersections where the traffic volume is low on cross streets. This research proposes a mathematical optimization model to enable uneven double cycling (UDC) in arterial signal coordination to address this issue. The model presents an equation for delay estimation when using double cycling and formulated a bi-objective optimization problem that maximizes bandwidth efficiency and minimize total average delay. The model introduces the concept of nominal red to describe the bandwidth geometry that is compatible with conventional arterial coordination. Through disjunctive programming techniques, the resultant model is a mixed integer quadratic programming problem with linear constraints. Based on numerical experiments evaluating the model performance, the research suggests several criteria for preliminary UDC application guidance. The UDC control scheme generally performs better at intersections with permitted left turn operation. When the arterial green time ratio between the minor intersection and the critical intersection under single cycling is greater than 2.06, the UDC control scheme is recommended for it can reduce delay without reducing bandwidth efficiency when compared with conventional single cycling. Following the preliminary guidelines, the case study using an actual field dataset showed promising results.

17. Key Words	18. Distribution Statement
Traffic Signals, Optimization, Progression, Coordination	No restrictions. This document is available to the public through NTIS: National Technical Information Service 5285 Port Royal Road Springfield, Virginia 22161

19. Security Classif.(of this report)	20. Security Classif.(of this page)	21. No. of Pages	22. Price
Unclassified	Unclassified	38	

ARTERIAL SIGNAL COORDINATION WITH UNEVEN DOUBLE CYCLING

by

Hongmin Zhou
Graduate Research Assistant
Texas A&M Transportation Institute

and

H. Gene Hawkins, Jr., Ph.D, P.E.
Associate Professor
Zachry Department of Civil Engineering
Texas A&M University

SWUTC/15/600451-00024-1

Sponsored by

Southwest Region University Transportation Center
Texas A&M University

January 2015

DISCLAIMER

The contents of this report reflect the views of the authors, who are responsible for the facts and the accuracy of the information presented herein. This document is disseminated under the sponsorship of the interest of information exchange. The U.S. Government assumes no liability for the contents or use itself.

ACKNOWLEDGEMENTS

The authors recognize that support for this work was provided by a grant from the U.S. Department of Transportation, University Transportation Centers Program to the Southwest Region University Transportation Center. The authors gratefully acknowledge Dr. Nadeem Chaudhary and Dr. Luca Quadrifoglio for their guidance on this research, Mr. John Black, Mr. Wayne Kurfees, and Dr. Tom Urbanik for their suggestions on initializing this research topic. In addition, special acknowledgements go to Dr. Xiaosi Zeng and Dr. Kai Yin for their participation in the discussions that inspired solutions to some of the problems encountered in the course of this research.

EXECUTIVE SUMMARY

In arterial coordination, high traffic volume at large intersections often requires a long cycle length to achieve good two-way progression. This long cycle length, however, often causes excessive delay at some minor intersections where the traffic volume is low on cross streets. This research proposes a mathematical optimization model to enable uneven double cycling (UDC) in arterial signal coordination to address this issue. The model presents an equation for delay estimation when using double cycling and formulated a bi-objective optimization problem that maximizes bandwidth efficiency and minimize total average delay. The model introduces the concept of nominal red to describe the bandwidth geometry that is compatible with conventional arterial coordination. Through disjunctive programming techniques, the resultant model is a mixed integer quadratic programming problem with linear constraints. Based on numerical experiments evaluating the model performance, the research suggests several criteria for preliminary UDC application guidance. The UDC control scheme generally performs better at intersections with permitted left turn operation. When the arterial green time ratio between the minor intersection and the critical intersection under single cycling is greater than 2.06, the UDC control scheme is recommended for it can reduce delay without reducing bandwidth efficiency when compared with conventional single cycling. Following the preliminary guidelines, the case study using an actual field dataset showed promising results.

TABLE OF CONTENTS

LIST OF FIGURES

LIST OF TABLES

CHAPTER 1. INTRODUCTION

BACKGROUND

As traffic volume has increased over the past two decades, the total hours of national urban traffic delay has almost doubled. Traffic agencies are using long cycle lengths (often over 150 seconds) during peak hours to provide adequate two-way arterial progression between large major-major intersections (high-volume on both roads) and to alleviate congestion at the critical intersections. However, conventional arterial coordination using a long cycle length can cause excessive delay for drivers on the minor cross streets at major-minor intersections (low-volume on the minor street). Traffic agencies have used half of the background cycle length at some of these major-minor intersections, where the second half cycle repeats exactly the same services (phasing sequences and splits) as the first half cycle, to reduce delay. With the introduction of 16-phase controllers, Kurfees proposed to address this issue with a more flexible tool, the "*uneven double cycling*" (UDC) control scheme (*1*), where the key phases in a cycle are unevenly repeated twice during the background cycle. Figure 1 shows two examples of the phase sequences and splits using an UDC scheme.

The UDC scheme shown in Figure 1 services all through movements twice (typically unequally) and typically services the protected left-turn (if any) once per background cycle at the minor intersections. Compared with half cycling, the UDC scheme is able to reduce delay on minor cross streets without impeding the passage of the green band in either direction on the arterial street, and is potentially applicable to more traffic and geometric scenarios. At present, the UDC control scheme are implemented at selected intersections in several cities (Richardson, Garland, Dallas, Houston) of Texas.

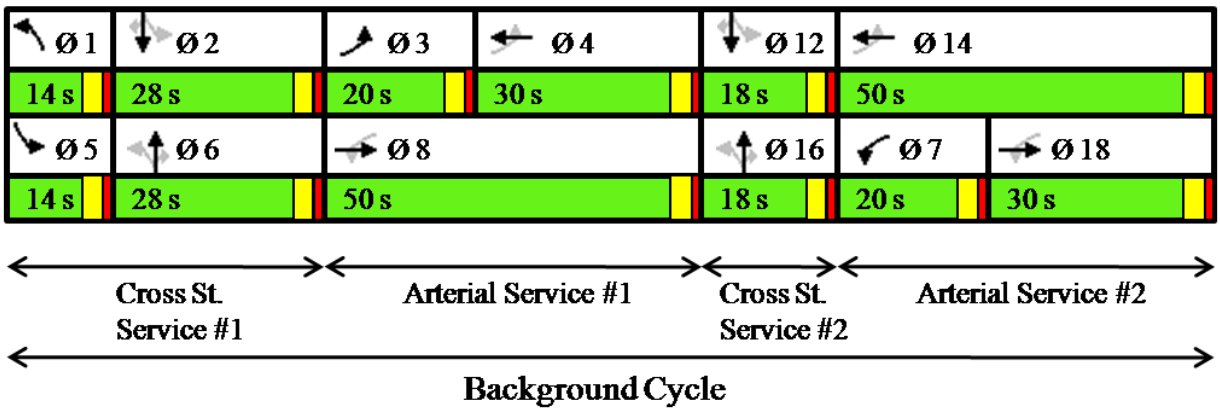

1a. UDC example with protected left turn on both streets

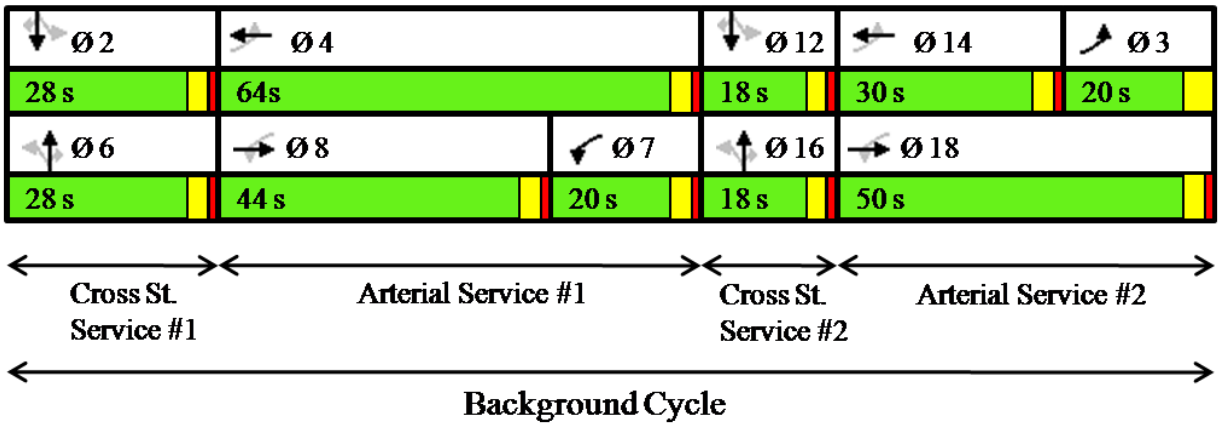

1b. UDC example with protected left turn on arterial only

Figure 1. Phase sequence and splits using an UDC scheme

RESEARCH OBJECTIVES AND TASKS

The goal of this research is to develop a mathematical model that generates arterial coordination signal timing plans with the UDC control scheme and provide preliminary guidelines for implementation. Research tasks include (1) a thorough literature review on arterial signal coordination methods, (2) developing a mathematical optimization model that enables uneven double cycling based on the MAXBAND program, (3) conducting numerical experiments and a case study to evaluate the performance of the model, and (4) providing preliminary implementation guidance for the UDC control scheme.

LITERATURE REVIEW

The UDC timing scheme has been developed manually in SYNCHRO (1, *2*) and thus might not be optimal, and few studies have addressed mathematical methods of optimizing coordination considering UDC control. Conventional off-line arterial signal optimization programs fall into three categories: bandwidth-based models, delay/stop-based models, and multiobjective models.

The bandwidth-based models e.g., MAXBAND and PASSER, are initially introduced by Morgan and Little (*3*) and generate the cycle lengths, offsets, and phase sequences to maximize the sum of directional green bands for progression (*4*). Extensive research efforts have been made to improve the bandwidth-based programs. Gartner *et al* (*5*) developed MULTIBAND to generate variable bandwidth for both directions to accommodate various traffic on different links. Tian and Urbanik (*6*) proposed a scheme to maximize bandwidth for the dominant direction and provide sufficiently large bandwidths within individual subsets of intersections on the other direction to ensure progression quality for arterials with large number of intersections. Chaudhary *et al*. (*7*) proposed a circular phasing scheme that services movements on four approaches clockwise or counter-clockwise in a four-phase sequence (main1-cross1-main2-cross2) to increase bandwidth. The delay/stop-based programs, e.g., TRANSYT-7F (*8*), minimize the linear combination of delay and stops by optimizing cycle length, green split, offset, and phase sequences. The bandwidth-based programs oversimplify traffic flow condition in the modeling and may result in unnecessary delay for cross-street traffic, whereas the delay/stop-based programs often do not produce good progression bands. As a consequence, researchers have made efforts in combining the merits of both types of methods to provide good progression and minimal delay (*9, 10, 11, 12*). However, none of these programs are capable of producing conditional services such as an uneven double cycling. This research proposed a UDC-enabled arterial coordination optimization method that maximizes two-way progression and minimizes signal delay.

CHAPTER 2. OPTIMIZATION MODEL

MODEL ASUMPTIONS

This research adopts the bandwidth geometry described in the MAXBAND program and utilizes the multiobjective optimization strategy to enable the double cycling capability. The model is based on the following assumptions:

1. Prevailing traffic conditions are under-saturated;
2. No lane blockage or spillback occurs for left turn or through movement;
3. Arriving and discharging traffic flow rates on all approaches are constant;

The three assumptions are intended to describe stable and recurring arterial traffic operation conditions for the optimization model to be applicable. Usually, the under-saturation assumption is met by using a long cycle length to achieve a volume-to-capacity ratio between 0.8 and 0.9 at the critical (often the major-major) intersection. This long background cycle length results in even smaller volume-to-capacity ratio at the major-minor intersections where the UDC scheme might be beneficial. Given enough turning bay length and link length, the assumption of no blockage or spillback can be satisfied. The constant flow assumption is to simplify delay estimation for computation efficiency.

Compared with conventional signal timing, uneven double cycling needs a different design of ring-barrier diagram and has more complicated bandwidth geometry. This section introduces mathematical formulations that are different from MAXBAND programming. The objective function involves delay estimation that is quadratic, but the constraints, through disjunctive programming, are still linear.

OBJECTIVE FUNCTION

The proposed model considers two objectives: the maximal two-way progression and the minimal total average delay. For simplicity, delay estimation only considers the uniform delay and applies the queuing diagram to derive the delay formula for a double cycled intersection (thus the under-saturated assumption).

Define that one sub-cycle consists of two consecutive sets of services each for traffic on the arterial and the cross street, and thus a background cycle has two sub-cycles (e.g., cross street service #1 and arterial service #1 make a sub-cycle in Figure 1). Also define the sub-cycle containing the outbound green band as the first sub-cycle $C1$ and thus the one without outbound green band as the second sub-cycle $C2$. Then the green split and red split for through movement in $C1$ are defined as first sub-green split $g1$ and first sub-red split $r1$, and the second sub-green split $g2$ and sub-red splits $r2$ are accordingly defined. With a given list of double-cycled intersections, for the j^{th} through movement at the u^{th} double cycled intersection, there exists two possible queuing diagrams as shown in Figure 2, depending on whether the first sub-green time is large enough to discharge vehicles queuing in the first sub-cycle. Given the assumption of constant flow, average delay per background cycle for this through movement is then calculated

using Equation 1. Definitions for terms used in all equations are contained at the end of the report.

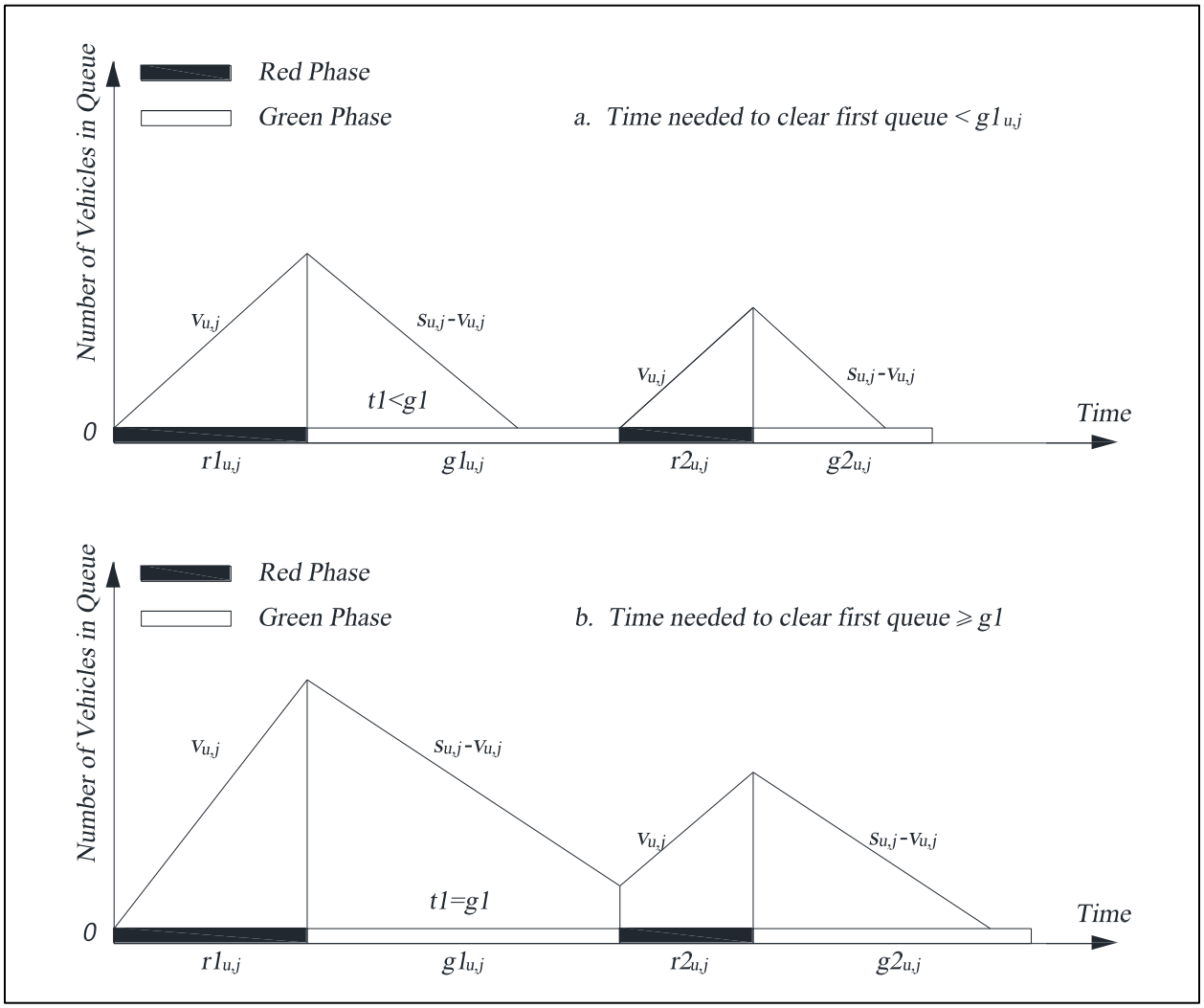

Figure 2. Queuing Diagram for at a Double Cycled Intersection

$$D_{u,j}^{Td} = \begin{cases} \dfrac{(r1_{u,j}^2 + r2_{u,j}^2)}{2(1-y_{u,j}^T)z} & if \quad \dfrac{r1_{u,j}}{1/y_{u,j}^T - 1} < g1_{u,j} \\ \dfrac{(r1_{u,j} + r2_{u,j})^2}{2(1-y_{u,j}^T)z} - \dfrac{r2_{u,j}\, g1_{u,j}}{y_{u,j}^T z} & if \quad \dfrac{r1_{u,j}}{1/y_{u,j}^T - 1} \geq g1_{u,j} \end{cases} \qquad \text{(Equ. 1)}$$

Equation 1 is equivalent to Equation 2.

$$D_{u,j}^{Td} = \frac{(r1_{u,j} + r2_{u,j})^2}{2(1-y_{u,j}^T)z} - \frac{t1_{u,j}\, r2_{u,j}}{y_{u,j}^T z} \qquad \text{(Equ. 2)}$$

Where $t1_{u,j}$ is the actual queue discharge time in the first sub-cycle $C1$ and is calculated using Equation 3.

$$t1_{u,j} = \min\{\frac{r1_{u,j}}{1/\ y_{u,j}^{T} - 1},\ g1_{u,j}\} \quad \text{(Equ. 3)}$$

Delay estimation of once-serviced movements (left turn movement for all approaches at all intersections and through movement for all approaches at single cycled intersections) are provided in Equations 4 and 5.

$$D_{i,j}^{L} = \frac{(1-l_{i,j})^2}{2(1-y_{i,j}^{L})z} \quad \text{(Equ. 4)}$$

$$D_{s,j}^{Ts} = \frac{(1-g_{s,j}^{s})^2}{2(1-y_{s,j}^{T})z} \quad \text{(Equ. 5)}$$

Summation of the three overall intersections and movements gives the total average delay as shown by Equation 6:

$$TD = \sum_{i=1}^{N}\sum_{j=1}^{J} D_{i,j}^{L} + \sum_{s=1}^{Ns}\sum_{j=1}^{J} D_{s,j}^{Ts} + \sum_{u=1}^{Nu}\sum_{j=1}^{J} D_{u,j}^{Td} \quad \text{(Equ. 6)}$$

Normalize respective objectives using bandwidth $BW_{\max}$ and delay $TD_{\max}$ resulted from MAXBAND program under single cycling as indicated by Equations 7 and 8.

$$BW_n = \frac{BW}{BW_{\max}} = \frac{cb_1 + (1-c)b_2}{BW_{\max}} \quad \text{(Equ. 7)}$$

$$TD_n = \frac{TD}{TD_{\max}} \quad \text{(Equ. 8)}$$

With λ^o being the weight of bandwidth, the objective function is the weighted sum of the opposite of normalized bandwidth and normalized total average delay as indicated in Equation 9.

$$\min:\ \ \lambda^o(-BW_n) + (1-\lambda^o)TD_n \quad \text{(Equ. 9)}$$

CONSTRAINTS

New constraints introduced in this model are mainly for describing the new bandwidth geometry and enabling selection of one of the sub-green phases for green band passage.

Sub-phase Splits and Timing Synchronization

The objective function involves calculating the sub-red splits for all approaches at a double cycled intersection. Both left-turn phase duration and left-turn patterns affect the sub-red time of through movement at a double cycled intersection. The left turn pattern depends on which of the two sub-cycles the left turn chooses and whether the left turn leads or lags in that sub-cycle.

With $\theta_{u,j}$ being the binary variable for protected left turn to select a sub-cycle, and $R1_{u,ja}(R2_{u,ja})$ being the total phase splits in the first (second) sub-cycle on the cross street, Table 1 and Equation 10 through Equation 14 show the determination of sub-red splits for arterial through phases. Calculation of sub-red splits of cross-street through movements follows the same method. Readers please refer to the glossary in alphabetical order at the end of the paper for term definitions.

Table 1. Left turn patterns and sub-red splits of arterial through movements

Left Turn Pattern	$\theta_{u,1}(\theta_{u,2})$	$\delta_{u,1}(\delta_{u,2})$	$r1_{u,1}(r1_{u,2})$	$r2_{u,1}(r2_{u,2})$
Left turn leads in $C1_u$	1	0	$r1_{u,ja} = R1_{u,ja} + L_{u,3-ja}$	$r2_{u,ja} = R2_{u,ja}$
Left turn lags in $C2_u$	0	1		
Left turn lags in $C1_u$	1	1	$r1_{u,ja} = R1_{u,ja}$	$r2_{u,ja} = R2_{u,ja} + L_{u,3-ja}$
Left turn leads in $C2_u$	0	0		

$$r1_{u,ja} = R1_{u,ja} + |\theta_{u,3-ja} - \delta_{u,3-ja}| L_{u,3-ja} \quad \text{(Equ. 10)}$$

$$r2_{u,ja} = R2_{u,ja} + (1 - |\theta_{u,3-ja} - \delta_{u,3-ja}|) L_{u,3-ja} \quad \text{(Equ. 11)}$$

Where:

$$R1_{u,ja} = g1_{u,ja+2} + 2Y + \theta_{u,5-ja} L_{u,5-ja} \quad \text{(Equ. 12)}$$

$$R2_{u,ja} = g2_{u,ja+2} + 2Y + (1 - \theta_{u,5-ja}) L_{u,5-ja} \quad \text{(Equ. 13)}$$

$$L_{u,j} = \begin{cases} (l_{u,j} + Y)\beta_u^a & if\ j = ja = 1,2 \\ (l_{u,j} + Y)\beta_u^c & if\ j = jc = 3,4 \end{cases} \quad \text{(Equ. 14)}$$

Substituting the sub-red splits into the objective function may affect the convexity of it because of the absolute function. This is improved by replacing the absolute function with a binary variable $\alpha_{u,j}^{I1}$ as indicated in Equation 15, where:

$$\alpha_{u,j}^{I1} = |\theta_{u,j} - \delta_{u,j}| \quad \text{(Equ. 15)}$$

Using a large value of $M = \frac{5}{2}$, this disjunctive constraint is equivalent to Equation 16.

$$\begin{cases} \alpha_{u,j}^{I1} - \theta_{u,j} + \delta_{u,j} \le \frac{5}{2}(1-\lambda_{u,j}^{D1}) \\ -\alpha_{u,j}^{I1} + \theta_{u,j} - \delta_{u,j} \le \frac{5}{2}(1-\lambda_{u,j}^{D1}) \\ \theta_{u,j} - \delta_{u,j} \le \frac{5}{2}(1-\lambda_{u,j}^{D1}) \\ \alpha_{u,j}^{I1} + \theta_{u,j} - \delta_{u,j} \le \frac{5}{2}\lambda_{u,j}^{D1} \\ -\alpha_{u,j}^{I1} - \theta_{u,j} + \delta_{u,j} \le \frac{5}{2}\lambda_{u,j}^{D1} \\ -\theta_{u,j} + \delta_{u,j} \le \frac{5}{2}\lambda_{u,j}^{D1} \end{cases} \quad \text{(Equ. 16)}$$

This model adopts the Highway Capacity Manual (*13*) method to calculate the total green split of a through phase under double cycling. This is done by adding the extra lost time resulted from the addition of two phases (assuming same per-phase lost time for all through phases) as shown in Equation 17.

$$g_{u,j}^{d} = \frac{y_{u,j}^{T}[1-Y(Nc_u+2)]}{\sum_{cj=1}^{Nc_u} y_{u,cj}} \quad \text{(Equ. 17)}$$

Then the sum of the two sub-green splits equals this total green split as shown in Equation 18, and each of the sub-green splits should meet the minimum green requirements as indicated in Equation 19 and Equation 20.

$$g1_{u,j} + g2_{u,j} = g_{u,j}^{d} \quad \text{(Equ. 18)}$$

$$g1_{u,j} \ge g_{u,j}^{\min} \quad \text{(Equ. 19)}$$

$$g2_{u,j} \ge g_{u,j}^{\min} \quad \text{(Equ. 20)}$$

The determination of the actual queue discharge time using Equation 3 is also a disjunctive constraint. Using a large value of $M = 1$, it is equivalent to Equation 21.

$$\begin{cases} t1_{u,j} - \dfrac{r1_{u,j}}{1/y_{u,j}^{T} - 1} \le 0 \\ -t1_{u,j} + \dfrac{r1_{u,j}}{1/y_{u,j}^{T} - 1} \le 1 - \lambda_{u,j}^{D2} \\ \dfrac{r1_{u,j}}{1/y_{u,j}^{T} - 1} - g1_{u,j} \le 1 - \lambda_{u,j}^{D2} \\ t1_{u,j} - g1_{u,j} \le 0 \\ -t1_{u,j} + g1_{u,j} \le \lambda_{u,j}^{D2} \\ -\dfrac{r1_{u,j}}{1/y_{u,j}^{T} - 1} + g1_{u,j} \le \lambda_{u,j}^{D2} \end{cases} \quad \text{(Equ. 21)}$$

In each of the sub-cycles, two-way services (through and left turn movements) on the major street start and end simultaneously, so do the minor street services. For the first sub-green phase, Equation 22 hold:

$$\begin{cases} g1_{u,1} + \theta_{u,2} L_{u,2} = g1_{u,2} + \theta_{u,1} L_{u,1} \\ g1_{u,3} + \theta_{u,4} L_{u,4} = g1_{u,4} + \theta_{u,3} L_{u,3} \end{cases} \quad \text{(Equ. 22)}$$

Given the HCM (*13*) method distributing green splits, all other synchronization and summation to the background cycle length automatically hold.

Bandwidth Geometry

The bandwidth geometry of two paired single-cycled intersections is the same as the original MAXBAND formulation. When involving the UDC scheme, the bandwidth geometry becomes more complicated than conventional coordination because the green band can choose to pass through either one of the two sub-green phases. This makes the bandwidth geometry very complex with conventional definitions of timing parameters. This model introduces the concept of nominal red. Nominal red is the time range in a background cycle where a possible green band chooses not to pass. It equals the background cycle length minus the sub-green phase time chosen for green band passage. Figure 3 shows the bandwidth geometry at a double-cycled intersection *i* and a single-cycled intersection *i*+1 for example. While keeping the same definitions terms as the original MAXBAND programming in describing the bandwidth geometry, this model defines new parameters and variables for double cycled intersections to calculate the nominal red splits. Readers please refer to the glossary at the end of the paper for detailed term definitions.

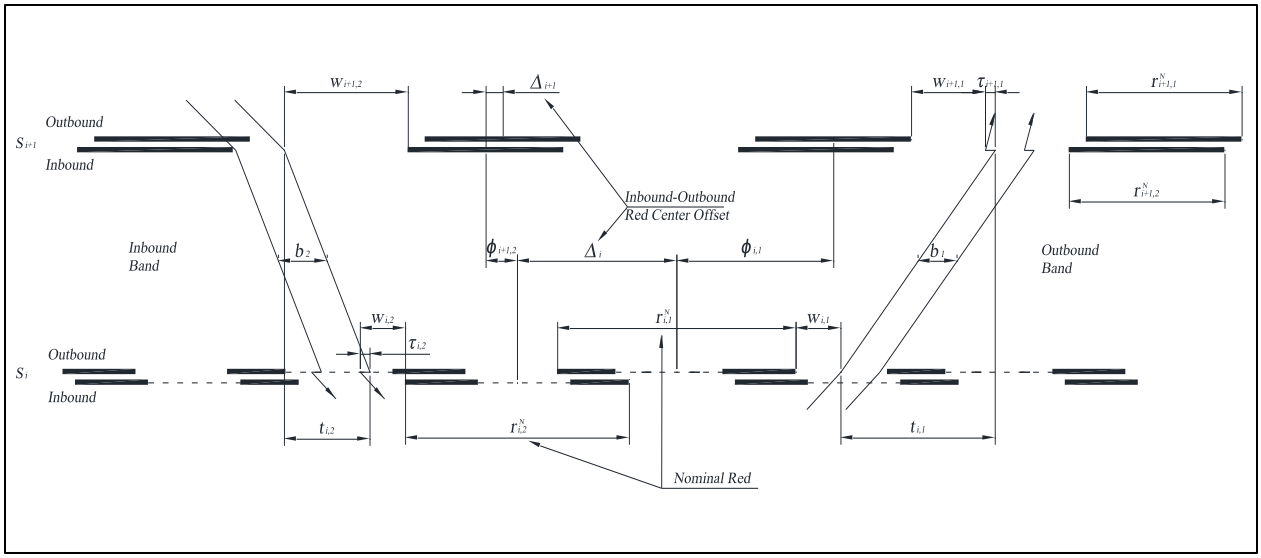

Figure 3. Bandwidth geometry at single- and double-cycled intersections

The green band of each direction can choose to pass only one of the two arterial through sub-green phases at the double-cycled intersection. The sub-green phase without green band passage lets traffic arriving after the end of the other sub-green phase. The two-way green bands could choose to pass a double cycled intersection through the same or different sub-green phases. Given the definition of the first sub-green phase, the inbound green band can choose to pass through either the first or the second sub-green phase. Therefore, the nominal red of a double cycled intersection of each arterial direction is determined using Equation 23 and 24 respectively. For a single cycled intersection, the nominal red follows the calculation of the conventionally defined red splits of arterial through movement.

$$r_{u,1}^{N} = 1 - g1_{u,1} \qquad \text{(Equ. 23)}$$

$$r_{u,2}^{N} = \begin{cases} 1 - g1_{u,2} & \text{if } b_2 \text{ chooses } g1_{u,2} \\ 1 - g2_{u,2} & \text{if } b_2 \text{ chooses } g2_{u,2} \end{cases} \qquad \text{(Equ. 24)}$$

Introducing the concept of nominal red allows the original definition of inbound and outbound red center offset Δ_i at a UDC intersection to be modified as the time from the center of inbound nominal red $r_{i,2}^{N}$ to the nearest center of outbound nominal red $r_{i,1}^{N}$. To facilitate the calculation of Δ_i, define that the outbound (inbound) arterial through sub-green of the green band starts at a time point $t_{i,1}^{o}(t_{i,2}^{o})$, and the difference between the two time points is $t_{i,1}^{o} - t_{i,2}^{o}$ (positive if the outbound coordinated green start point is to the right of the inbound coordinated green start point). Then Δ_i :is determined using Equation 25.

$$\Delta_i = t_{i,1}^{o} - t_{i,2}^{o} - \frac{1}{2}(r_{i,1}^{N} - r_{i,2}^{N}) \qquad \text{(Equ. 25)}$$

For a single-cycled intersection, Equation 26 applies.

$$\Delta_s = \frac{1}{2}[(2\delta_{s,1} - 1)L_{s,1} - (2\delta_{s,2} - 1)L_{s,2}] \quad \text{(Equ. 26)}$$

For double cycling, Table 2 and Equation 27 show the determination of $t_{u,1}^o - t_{u,2}^o$ in association with different left turn patterns at a double cycled intersection.

Table 2. Difference between the start time point of coordinated through green

Left Turn Pattern		$\theta_{u,1}$	$\theta_{u,2}$	$\delta_{u,1}$	$\delta_{u,2}$	$t_{u,1}^o - t_{u,2}^o$	
$L_{u,1}$	$L_{u,2}$					b_2 chooses $g1_{u,2}$	b_2 chooses $g2_{u,2}$
leads in $C1_u$	lags in $C1_u$	1	1	0	1	$-L_{u,1}$	$-(R2_{u,1} + g1_{u,1} + L_{u,2})$
lags in $C1_u$	leads in $C1_u$	1	1	1	0	$L_{u,2}$	$-(R2_{u,1} + g1_{u,1})$
leads in $C1_u$	leads in $C1_u$	1	1	0	0	$L_{u,2} - L_{u,1}$	$-(R2_{u,1} + g1_{u,1})$
lags in $C1_u$	lags in $C1_u$	1	1	1	1	0	$-(R2_{u,1} + g1_{u,1} + L_{u,2})$
leads in $C1_u$	lags in $C2_u$	1	0	0	1	$-L_{u,1}$	$-(R2_{u,1} + g1_{u,1})$
lags in $C1_u$	leads in $C2_u$	1	0	1	0	0	$-(R2_{u,1} + g1_{u,1})$
leads in $C1_u$	leads in $C2_u$	1	0	0	0	$-L_{u,1}$	$-(R2_{u,1} + g1_{u,1})$
lags in $C1_u$	lags in $C2_u$	1	0	1	1	0	$-(R2_{u,1} + g1_{u,1})$
leads in $C2_u$	lags in $C1_u$	0	1	0	1	0	$-(R2_{u,1} + g1_{u,1} + L_{u,1} + L_{u,2})$
lags in $C2_u$	leads in $C1_u$	0	1	1	0	$L_{u,2}$	$-(R2_{u,1} + g1_{u,1})$
leads in $C2_u$	leads in $C1_u$	0	1	0	0	$L_{u,2}$	$-(R2_{u,1} + g1_{u,1} + L_{u,1})$
lags in $C2_u$	lags in $C1_u$	0	1	1	1	0	$-(R2_{u,1} + g1_{u,1} + L_{u,2})$
leads in $C2_u$	lags in $C2_u$	0	0	0	1	0	$-(R2_{u,1} + g1_{u,1} + L_{u,1})$
lags in $C2_u$	leads in $C2_u$	0	0	1	0	0	$-(R2_{u,1} + g1_{u,1})$
leads in $C2_u$	leads in $C2_u$	0	0	0	0	0	$-(R2_{u,1} + g1_{u,1} + L_{u,1})$
lags in $C2_u$	lags in $C2_u$	0	0	1	1	0	$-(R2_{u,1} + g1_{u,1})$

$$t_{u,1}^o - t_{u,2}^o = \begin{cases} (-\theta_{u,1} + \theta_{u,1}\delta_{u,1})L_{u,1} + (\theta_{u,2} - \theta_{u,2}\delta_{u,2})L_{u,2} & \text{if } b_2 \text{ chooses } g1_{u,2} \\ -[R2_{u,1} + g1_{u,1} + (1 - \theta_{u,1} - \delta_{u,1} + \theta_{u,1}\delta_{u,1})L_{u,1} + \theta_{u,2}\delta_{u,2}L_{u,2}] & \text{if } b_2 \text{ chooses } g2_{u,2} \end{cases} \quad \text{(Equ. 27)}$$

Eliminate nonlinearity in Equation 27 by replacing the product of the two binary variables $\theta_{u,ja}\delta_{u,ja}$ with a new binary variable $\alpha_{u,ja}^{I2}$ as shown in Equation 28, where:

$$\alpha_{u,ja}^{I2} = \theta_{u,ja}\delta_{u,ja} \quad \text{(Equ. 28)}$$

Which is equivalent to Equation 29.

$$\begin{cases} \alpha_{u,ja}^{I2} + \theta_{u,ja} + \delta_{u,ja}^{d} - 3 \le \frac{3}{2}(1 - \lambda_{u,ja}^{D3}) \\ -\alpha_{u,ja}^{I2} - \theta_{u,ja} - \delta_{u,ja}^{d} + 3 \le \frac{3}{2}(1 - \lambda_{u,ja}^{D3}) \\ \alpha_{u,ja}^{I2} + \theta_{u,ja} + \delta_{u,ja}^{d} - 2 \le \frac{3}{2}\lambda_{u,ja}^{D3} \\ \alpha_{u,ja}^{I2} \le \frac{3}{2}\lambda_{u,ja}^{D3} \\ -\alpha_{u,ja}^{I2} \le \frac{3}{2}\lambda_{u,ja}^{D3} \end{cases} \quad \text{(Equ. 29)}$$

Linearize the calculation of inbound nominal red $r_{u,2}^{N}$ and red-center offset Δ_u through disjunctive programming again using Equation 30 and Equation 31:

$$\begin{cases} r_{u,2}^{N} - 1 + g1_{u,2} \le 1 - \lambda_u^{D4} \\ -r_{u,2}^{N} + 1 - g1_{u,2} \le 1 - \lambda_u^{D4} \\ r_{u,2}^{N} - 1 + g2_{u,2} \le \lambda_u^{D4} \\ -r_{u,2}^{N} + 1 - g2_{u,2} \le \lambda_u^{D4} \end{cases} \quad \text{(Equ. 30)}$$

$$\begin{cases} \Delta_u - (-\theta_{u,1} + \alpha_{u,1}^{I2})L_{u,1} - (\theta_{u,2} - \alpha_{u,2}^{I2})L_{u,2} + \frac{1}{2}(r_{u,1}^{N} - r_{u,2}^{N}) \le \frac{11}{2}(1 - \lambda_u^{D4}) \\ -\Delta_u + (-\theta_{u,1} + \alpha_{u,1}^{I2})L_{u,1} + (\theta_{u,2} - \alpha_{u,2}^{I2})L_{u,2} - \frac{1}{2}(r_{u,1}^{N} - r_{u,2}^{N})] \le \frac{11}{2}(1 - \lambda_u^{D4}) \\ \Delta_u + g2_{u,3} + 2Yz + (1 - \theta_{u,4})L_{u,1} + g1_{u,1} + (1 - \theta_{u,1} - \delta_{u,1} + \alpha_{u,1}^{I2})L_{u,1} \\ \qquad + \alpha_{u,2}^{I2}L_{u,2} + \frac{1}{2}(r_{u,1}^{N} - r_{u,2}^{N}) \le \frac{11}{2}\lambda_u^{D4} \\ -\Delta_u - g2_{u,3} - 2Yz - (1 - \theta_{u,4})L_{u,1} - g1_{u,1} - (1 - \theta_{u,1} - \delta_{u,1} + \alpha_{u,1}^{I2})L_{u,1} \\ \qquad - \alpha_{u,2}^{I2}L_{u,2} - \frac{1}{2}(r_{u,1}^{N} - r_{u,2}^{N}) \le \frac{11}{2}\lambda_u^{D4} \end{cases} \quad \text{(Equ. 31)}$$

Other constraints in the original MAXBAND program remain the same as shown in Equation 32 through Equation 36, except that conventionally defined red split was replaced with the nominal red split accordingly.

$$\begin{aligned} &(w_{i,1} + w_{i,2}) - (w_{i+1,1} + w_{i+1,2}) + (t_{i,1} + t_{i,2}) + \Delta_i - \Delta_{i+1} - m_i \\ &\qquad = -\frac{1}{2}(r_{i,1}^{N} + r_{i,2}^{N}) + \frac{1}{2}(r_{i+1,1}^{N} + r_{i+1,2}^{N}) + (\tau_{i,1} + \tau_{i,2}) \end{aligned} \quad \text{(Equ. 32)}$$

$$-kb_1 + b_2 \begin{cases} = 0 \ \ if \ \ k = 1 \\ \ge 0 \ \ if \ \ k < 1 \\ \le 0 \ \ if \ \ k > 1 \end{cases} \quad \text{(Equ. 33)}$$

$$w_{i,ja} + b_{ja} \le 1 - r_{i,ja}^{N} \quad \text{(Equ. 34)}$$

$$(\frac{d_{i,ja}}{f_{i,ja}})z \le t_{i,ja} \le (\frac{d_{i,ja}}{e_{i,ja}})z \quad \text{(Equ. 35)}$$

$$(\frac{d_{i,ja}}{h_{i,ja}})z \le (\frac{d_{i,ja}}{d_{i+1,ja}})t_{i+1,ja} - t_{i,ja} \le (\frac{d_{i,ja}}{o_{i,ja}})z \quad \text{(Equ. 36)}$$

In comparison to the mixed integer linear programming used in the original problem, the resultant model is a mixed integer quadratic programming (MIQP) problem due to the existence of quadratic components of delay estimation in the objective function. The optimization process follows the steps below. If a list of UDC intersections were available before hand, step 2 can be skipped:

1. Run MAXBAND model to produce maximum bandwidth and delay under single cycling;
2. Run the proposed model by trying double cycling one intersection at a time with $\lambda^o = 1$ for all noncritical intersections; choose those giving BW_{nor} that is greater than a prescribed threshold to determine a list of UDC intersections.
3. Use the list of UDC intersections and varied λ^o to rerun the proposed model until a preferred combination of BW_{nor} and TD_{nor} is reached.

CHAPTER 3. NUMERICAL EXPERIMENTS AND CASE STUDY

NUMERICAL EXPERIMENTS

Factors affecting UDC application may include through and left turn volume levels on both arterial and cross streets, capacity of different lane groups, distance between intersections, traffic differences between major-major and major-minor intersections, and traffic differences between arterial streets and minor cross streets at the major-minor intersections, among other factors. Exploratory analyses indicated that the model performance is sensitive to parameters calculated using volume-to-saturation flow ratio (*v/s*), therefore we used several of these parameters to test the model trying to find certain traffic thresholds and develop preliminary criteria for UDC implementation guidance.

Experiment Design

To find the effective indicators for UDC application, we considered three sets parameters: (1) left turn percentage on the arterial and minor cross streets; (2) traffic ratio between arterial streets and minor cross streets at the double-cycled intersections; and (3) traffic difference between double-cycled and single-cycled intersections. Each of them is discussed as follows.

Left turn percentage on an approach was calculated as the left turn *v/s* ratio on this approach divided by the sum of this left turn v/*s* and the opposing through *v/s*. Left turn percentage on the critical approach of arterial (*ArtLT*) and of cross streets (*CrstLT*) were used as a set of controlling parameters for a candidate UDC intersection. The two parameters actually reflected the weight of through movement in demand of green time allocation. Numeric experiments considered protected left turn only on the arterial and protected or permitted left turn on cross streets. Both *ArtLT* and *CrstLT* ranged from one percent to 70 percent.

Traffic ratio between arterial streets and cross streets (*AtC*) was defined as the ratio between the sum of critical *v/s* for arterial phases and the sum of critical *v/s* for cross-street phases. This parameter reflected the relative demand in green time allocation on arterial and cross streets. *AtC* ranged from 0.5 to 0.9 in the numeric experiments.

We investigated three parameters for traffic difference between single cycled and double cycled intersections. Arterial traffic ratio between double and single cycled intersections (*UtS*) was defined as the ratio of critical *v/s* for arterial phases between the candidate UDC intersection and the critical intersection in the arterial (the intersection dictating arterial background cycle length). This parameter served to generate various traffic flow levels at the UDC intersection in comparison with the critical single-cycled intersection. *UtS* ranged from 0.8 to 1.2 in the numeric experiments. The second parameter was the ratio of volume-to-capacity ratio (*Xc*) between candidate UDC and the critical intersections (*Xc-ratio*). This parameter reflected comprehensively traffic demand and supply for both intersections. Another parameter investigated in the study was the arterial green time ratio between candidate UDC intersection and the critical intersection under single cycling (*g-ratio*). It was calculated as the average of the

outbound and inbound ratios. This was a more direct parameter reflecting the applicability of UDC control scheme since changes in all other parameters eventually affect the optimization results through green splits on the arterial. Both *Xc-ratio* and *g-ratio* varied as a result of changes in all the other parameters.

We considered a hypothetical arterial with three intersections, where the two intersections at both ends were single-cycled and the one in between was an UDC candidate. The above parameters were varied to generate different flow levels for different movements at the candidate UDC intersection. Other parameters like background cycle length (C=160 sec) volume-to-capacity ratio (Xc=0.9 and 0.81) at single-cycled intersections, distance between intersections (1000 ft and 2000 ft), inbound and outbound relative flow ratios (0.3 on arterial streets, 0.85 on minor streets), and speed limit boundaries (40 mph ± 2.5 mph) were kept the same throughout the experiments. ILOG-CPLEX (*14*) was used to code and solve the model for its ability to solve global optimum of MIQP problems. The optimization model provided various bandwidth solutions, and the next section discusses the results. It should be noted that the numerical experiments were not designed to cover all possible traffic scenarios in discussing UDC applicability. Instead we determined ranges of the above parameters by first considering representing scenarios where UDC control might be beneficial and then varying the parameters within proper ranges to observe the model performance.

Experiment Results

This section first discussed qualitatively and quantitatively each of the above factors to see their impact on the bandwidth solutions and then gave preliminary criteria for UDC application guidance.

Before discussing the results, it is worth explaining the algorithm used in the model to calculate green splits when minimum green requirements are not met using the initial input flow information. The algorithm first calculates the initial *Xc* and the green splits using the input flow information. If the minimum green requirement are not met for a particular phase, *v/s* of this phase is increased by a small increment, and then *v/s* of each phase is updated by redistributing the new critical sum of *v/s* on a street according to the *v/s* in the last step, if necessary. A new *Xc* is then calculated using the updated flow information. This iteration goes until all phases meet the minimum green requirements. Delay calculation still uses the initial *v/s* ratios.

Left Turn Factors

Figure 4 shows the changes in normalized bandwidth efficiency as *CrstLT* and *ArtLT* change while fixing *UtS* and *AtC*. Figure 4a indicates that, as *CrstLT* increases, bandwidth gradually increases under permitted left turn operation but stays at approximately the same level before dropping sharply after *CrstLT* passes about 0.45 under protected left turn. Figure 4b shows that as *ArtLT* increases, bandwidth decreases under both permitted and protected left turn on cross streets. The UDC control scheme performs better for permitted left turn operations.

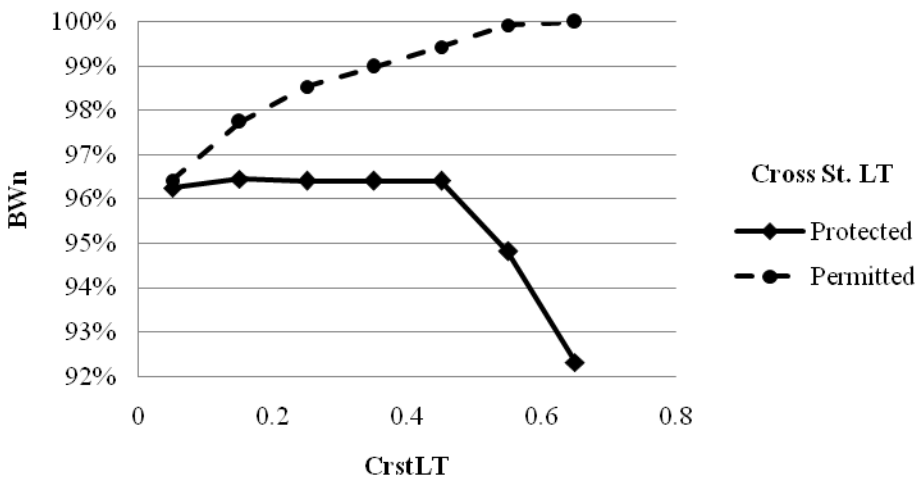

4a. *BWn* by *CrstLT* (*UtS*=1.0, *AtC*=0.7, *ArtLT*=0.01)

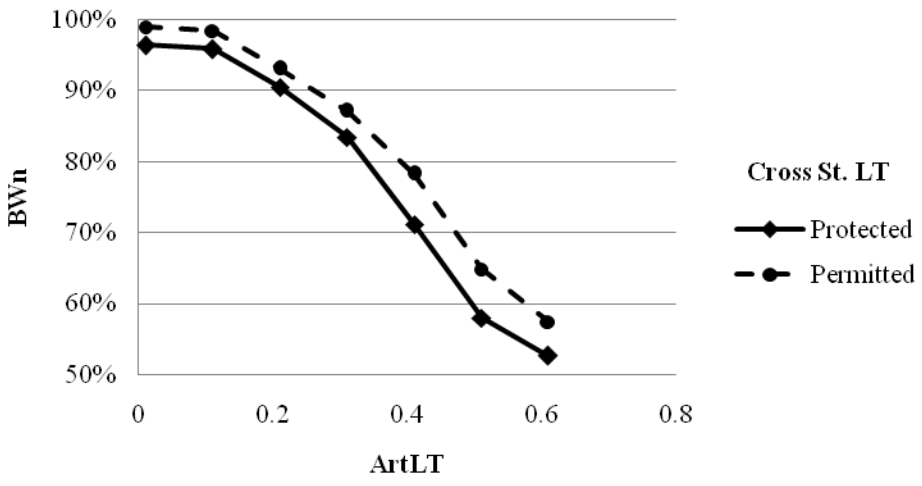

4b. *BWn* by *ArtLT* (*UtS*=1.0, *AtC*=0.7, *CrstLT*=0.35)

Figure 4. Bandwidth affected by different left turn percentages

For permitted left turn on cross streets, increasing *CrstLT* decreases *v/s* for through movements on cross streets which reduces the critical sum of *v/s* and thus *Xc* for the intersection. This increases green time allocation for arterial phases and thus available green time for progression.

For protected left turn on cross streets, changing *CrstLT* causes redistribution of phase splits depending on whether the minimum green requirements are met for left turn or through movements. When *CrstLT* is small and the initial phase split did not meet the minimum left turn requirement, the algorithm produces small *Xc* and thus large arterial through green splits for

progression. When *CrstLT* is high, increasing *CrstLT* reduces through phase splits on cross streets to be below minimum green. The algorithm generates large *Xc* and thus small arterial through green splits and bandwidth. When *CrstLT* is at medium levels, increasing *CrstLT* does not affect the sum of critical *v/s*, and therefore arterial phase splits and bandwidth remain the same.

Increasing *ArtLT* directly reduces through phase splits on arterial, and thus the available green time for progression decreases. This applies to both permitted and protected left turn operations on cross streets. The only difference is that under permitted left turn operation, the available green time for progression is greater than that under protected left turn operation, given all other factors the same.

Results for other *CrstLT* and *ArtLT* levels show similar trends except the curves lie at different levels of normalized bandwidth efficiency (see Figure 5). Each of the *BWn-CrstLT* curves lies in a narrow range of bandwidth efficiency (often within ten percent of range), whereas each of the *BWn-ArtLT* curves covers a wider range of bandwidth efficiency (often more than 40 percent of range). This indicates that a threshold of criteria might be better observed for *ArtLT* than *CrstLT* for UDC application guidance. Considering arterial progression quality being the first priority, we suggested that bandwidth efficiency with UDC be at least 90 percent of that under single cycling for being considered for the UDC control scheme. Therefore *ArtLT* has to be no greater than 0.21 according to the results. For permitted left turn operation on cross streets, *ArtLT* has to be no greater than 0.09 for the UDC model to reach the same bandwidth efficiency (*BWn* =100%) as single cycling. For protected left turn operation, *ArtLT* has to be no greater than 0.15 for the model to yield a bandwidth efficiency that was 97 percent or higher of that under single cycling.

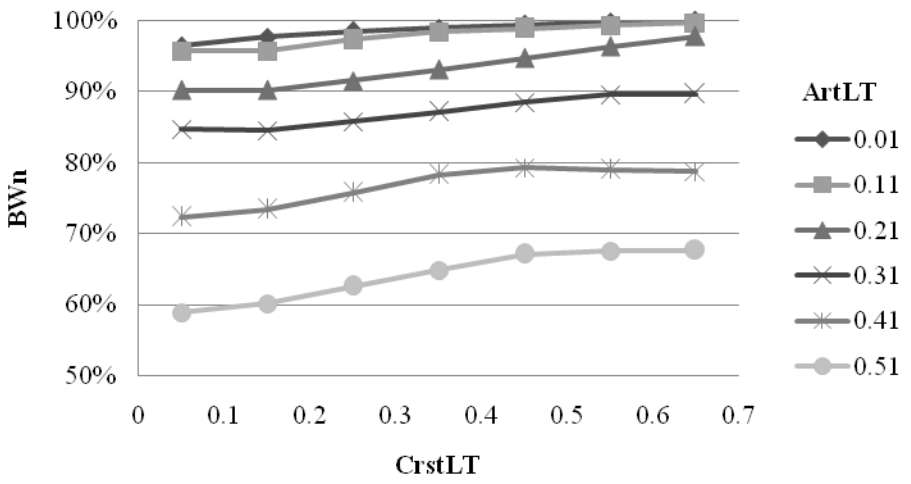

5a. Permitted left turn on cross streets (*UtS*=1.0, *AtC*=0.7)

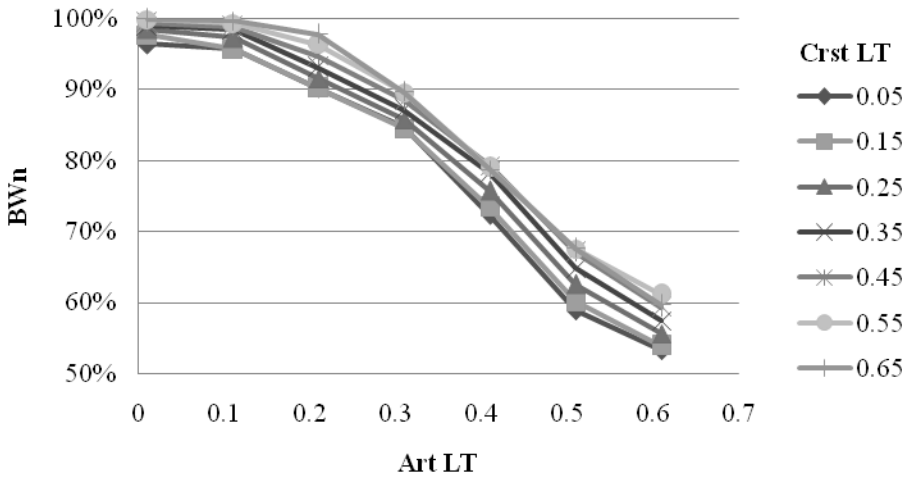

5b. *BWn* by *ArtLT* under different *CrstLT* levels (*UtS*=1.0, *AtC*=0.7)

Figure 5. Bandwidth affected by different left turn percentages for permitted left turn

Traffic Difference between Arterial and Cross Streets at Double-cycled Intersection

Figure 6 shows the changes in normalized bandwidth efficiency by *AtC* under different levels of left turn percentage for permitted left turn operation on cross streets (*UtS*=1.0, *CrstLT*=0.35). As *AtC* increases, bandwidth generally increases when *AtC* was greater than 0.65. When *AtC* is less than 0.65, bandwidth does not change very much. Similar to *ArtLT*, as *AtC* changes, each of the *BWn-AtC* curves covers a wide range of bandwidth efficiency, and part of which is monotone increasing. It is possible to observe threshold values of *AtC* for UDC implementation guidance. For permitted left turn operation on cross streets, *AtC* has to be no less than 0.7 for the UDC

model to yield the same bandwidth as single cycling. For protected left turn operation, *AtC* has to be no lower than 0.75 for the UDC model to provide a bandwidth efficiency that is 97 percent or higher of that under single cycling.

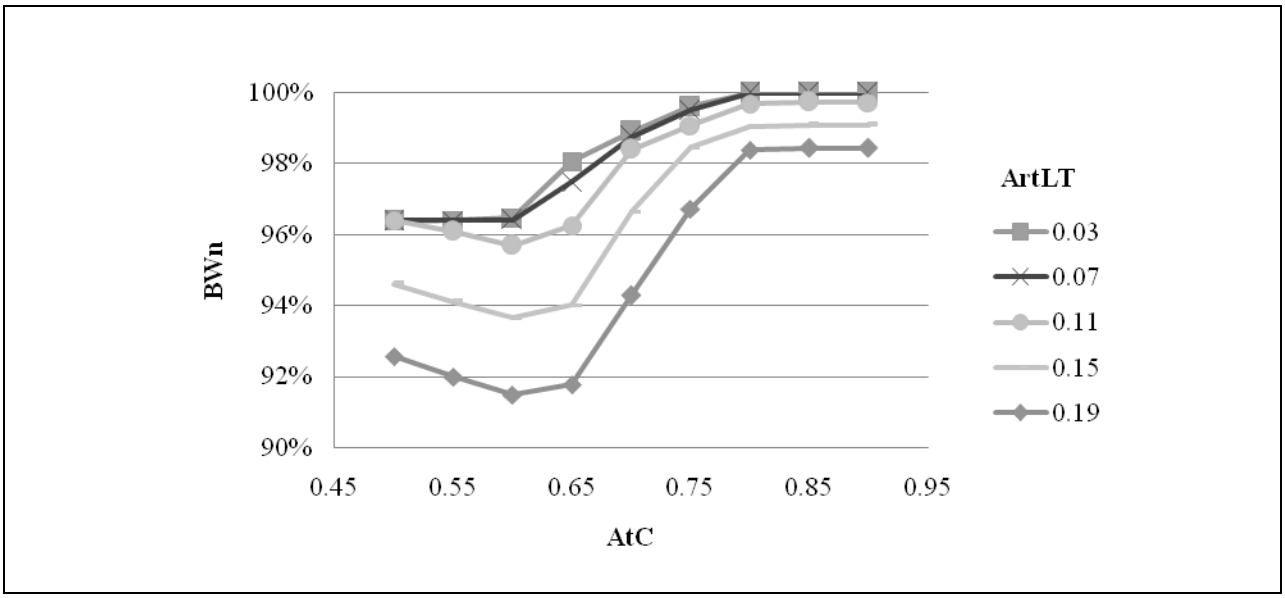

Figure 6. Bandwidth affected by *AtC* under permitted left turn operation

Traffic Difference between Double-cycled and Single-cycled Intersections

Bandwidth efficiency does not change very much as *UtS* varies given all other factors the same, and different levels of left turn percentages. This is because the experiment data is generated in a way that changing *UtS* alone does not change the relative traffic level among different movements on different streets at the UDC intersection, and thus does not necessarily change the green split allocation affecting UDC optimization results.

Figure 7 shows mixed results for the impact of *Xc-ratio* on UDC bandwidth efficiency. When only *AtC* varies, as seen in Figure 7a, *Xc-ratio* changes with *AtC*, and the normalized bandwidth efficiency varies within a range of three percent. When only *ArtLT* varies, as seen in Figure 7a, *Xc-ratio* does not necessarily changes with *ArtLT*. *BWn* could vary a lot at approximately the same *Xc-ratio* level (for example, *Xc-ratio*=0.80 in Figure 7b). *BWn* could also remain at the same level even when *Xc-ratio* varies a lot (for example, *BWn* stays at about 96.3% when *Xc-ratio* increases from 0.81 to 0.85 in Figure 7b). Therefore, *Xc-ratio* is not a sufficient indicator about whether the UDC control scheme would be beneficial for an intersection.

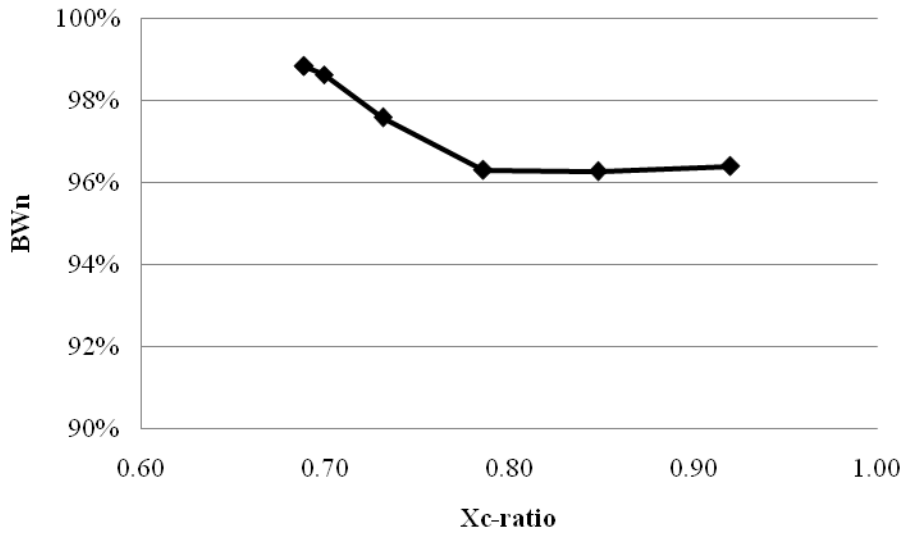

7a. *BWn* by *Xc-ratio* when only *AtC* varies (*CrstLT*=0.35, *UtS*=1.0, *ArtLT*=0.03)

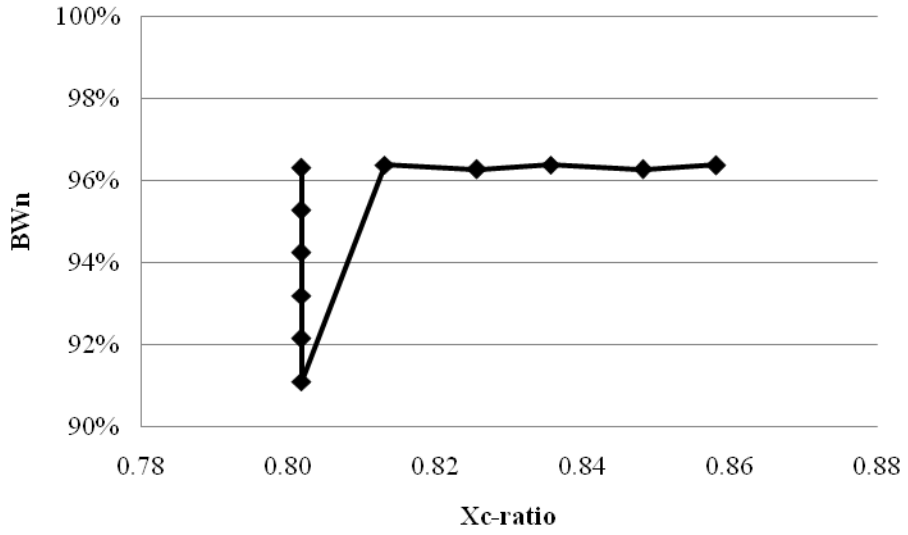

7b. *BWn* by *Xc-ratio* when only *ArtLT* varies (*CrstLT*=0.35, *UtS*=1.0, *AtC*=0.65)

Figure 7. Bandwidth affected by *Xc-ratio* under different scenarios

Figure 8 shows changes in normalized bandwidth efficiency by *g-ratio* under different levels of left turn percentage. For permitted left turn operation on cross streets, when *CrstLT* is 0.35 and above, the higher *g-ratio*, the greater bandwidth efficiency; when *CrstLT* is lower than 0.35, *BWn* first increases with *g-ratio* and then stays approximately at the same level after *g-ratio* passed certain value. For protected left turn on cross streets, when *g-ratio* is less than 1.45, *BWn* increases with *g-ratio*.

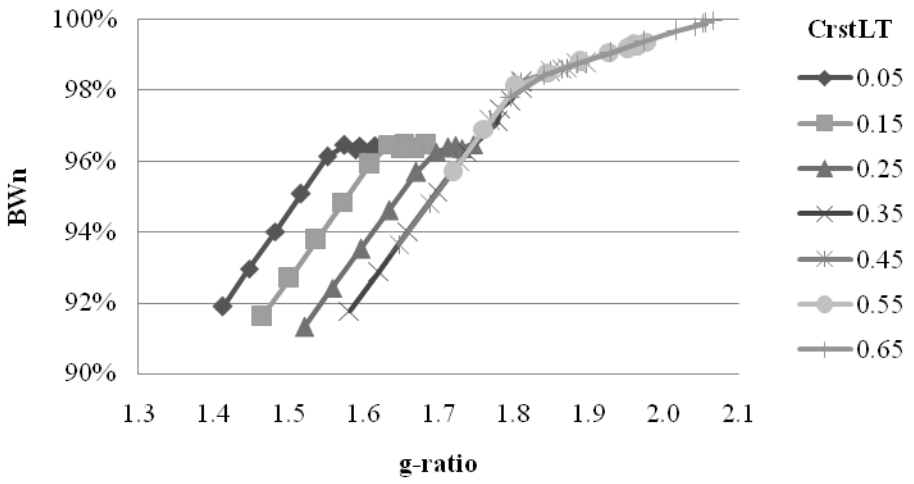

8a. Permitted left turn operation on cross streets (*AtC*=0.65)

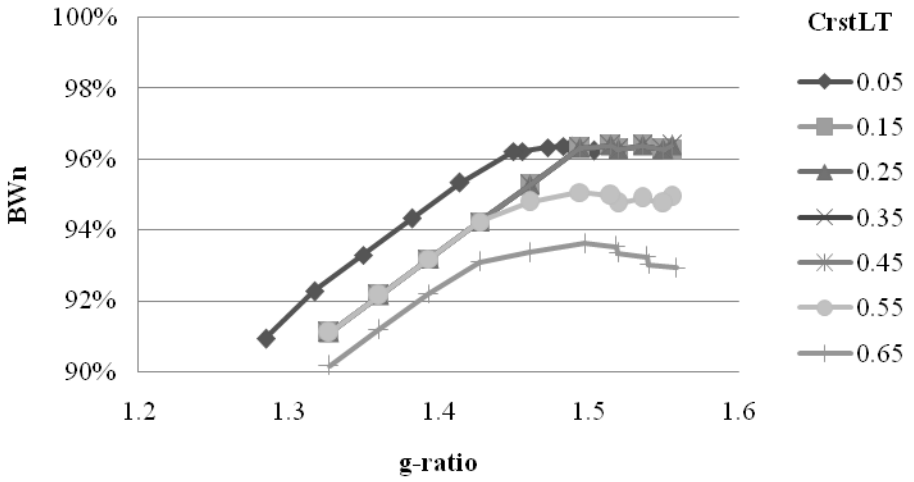

8b. Protected left turn operation on cross streets (*AtC*=0.65)

Figure 8. UDC Bandwidth by *UtS* under different *CrstLT* levels

Table 3 lists detailed thresholds of *g-ratio* for various *CrstLT* and *AtC* levels when UDC can provide bandwidth efficiency at least 95 percent of that under single cycling. For permitted left turn on cross streets, when *g-ratio* is 2.06 or higher the UDC control scheme can generate the same bandwidth efficiency as single cycling while saving 3.2 percent of average total delay. For protected left turn operation, *g-ratio* has to at least 1.77 for the UDC model to provide 97 percent or higher of bandwidth efficiency of that under single cycling while saving 3.4 percent average total delay. It is worth mentioning that determining the threshold of g-ratio largely depends on the required minimum green time for left turn and through phases. For this research, we used 10

sec and 15 sec for left turn and through movements on arterial respectively, and 7 sec and 10 sec on minor cross streets respectively.

Table 3. Thresholds of *g-ratio* when *BWn* is 95% or higher

	CrstLT	AtC								
		0.50	**0.55**	**0.60**	**0.65**	**0.70**	**0.75**	**0.80**	**0.85**	**0.90**
Permitted Left turn on cross streets	0.05	N/A*	1.29	1.40	1.52	1.67	1.70			
	0.15	1.26	1.35	1.46	1.61	1.72	1.70			
	0.25	1.31	1.42	1.53	1.67	1.70	1.71			
	0.35	1.39	1.50	1.64	1.70	1.71	1.76	1.73	1.83	1.93
	0.45	1.48	1.62	1.71	1.73	1.72	1.80			
	0.55	1.62	1.71	1.72	1.72	1.79	1.86			
	0.65	1.70	1.70	1.73**	1.80	1.86	1.91			
Protected Left turn on cross streets	0.05		N/A	1.31	1.41	1.55	1.66	1.73	1.75	1.84
	0.15		1.27	1.35	1.46	1.60	1.70	1.72	1.77	1.86
	0.25		1.27	1.35	1.46	1.61	1.72	1.72	1.80	1.88
	0.35	N/A	1.27	1.35	1.46	1.61	1.72	1.76	1.82	1.89
	0.45		1.27	1.35	1.46	1.61	1.72	1.80	1.82	1.89
	0.55		1.27	1.35	NA	NA	NA	1.80	1.86	1.88
	0.65		1.27	1.35	NA	NA	NA	1.84	1.87	1.86

Note: * N/A means either no solution or normalized bandwidth efficiency is less than 95%;
** The underlined figure indicates the lowest *g-ratio* when *ArtLT* is less than 0.20 can provide *BWn*≥0.95%.

CASE STUDY

After the numerical experiments, we conducted a case study using field data by first following the preliminary guidelines developed according to the results of numerical experiments and then running the UDC-enabled optimization model on the data to see the actual model results.

Field data for the case study are traffic (arriving flow and saturation flow adjusted according to HCM (*13*)) and geometric data of an arterial with four intersections (Campbell Rd from N Plano Rd to N Jupiter Rd) in Richardson, Texas. At both ends of the arterial were two major-major intersections requiring 160 sec for good two-way progression, while the two major-minor intersections in between experiences unnecessary delays under signal cycling. Table 4 shows the adjusted flow rate at each of the four intersections along this arterial during PM peak hours.

Table 4. Traffic flow (vph) data for case study

	EBL	EBT	EBR*	WBL	WBT	WBR	NBL	NBT	NBR	SBL	NBT	SBR
Jupiter	621	1267	320	135	335	0	286	1460	199	92	1217	73
Yale	82	2283	76	22	652	17	22	22	0	22	22	0
Owens	87	2272	87	54	587	39	43	43	0	43	43	0
Plano	224	1985	247	175	546	49	356	1264	295	318	1200	72

Note: * Right turn on red traffic has been deducted.

The two major-minor intersections are considered as the candidate UDC intersections. Both intersections have permitted left turn operation on the cross streets. Table 5 lists the calculated values of suggested parameters for checking UDC applicability criteria. The results indicates that UDC control might beneficial at both intersections for achieving the same bandwidth as single cycling (*BWn* = 100%) while reducing delay on the cross streets.

Table 5. Checking UDC application criteria for the case study

	ArtLT		AtC		g-ratio		UDC?
	Actual	Threshold	Actual	Threshold	Actual	Threshold	
Owens	0.06	<=0.09	0.93	>=0.7	2.13	>=2.06	Yes
Yale	0.03		0.95		2.17		Yes

We ran the optimization model on the data and the results are as expected. The model chooses double cycling at both of the major-minor intersections and achieves the same bandwidth as that of single cycling (*BWn* = 100%) while saving 4.3 percent of the total average delay (*TDn* = 95.7%). Figure 9 shows the time-space diagram of the model results. Intuitively, the model minimizes green splits close to minimum through green on cross streets in the sub-cycle without green band passage to reach the optimism.

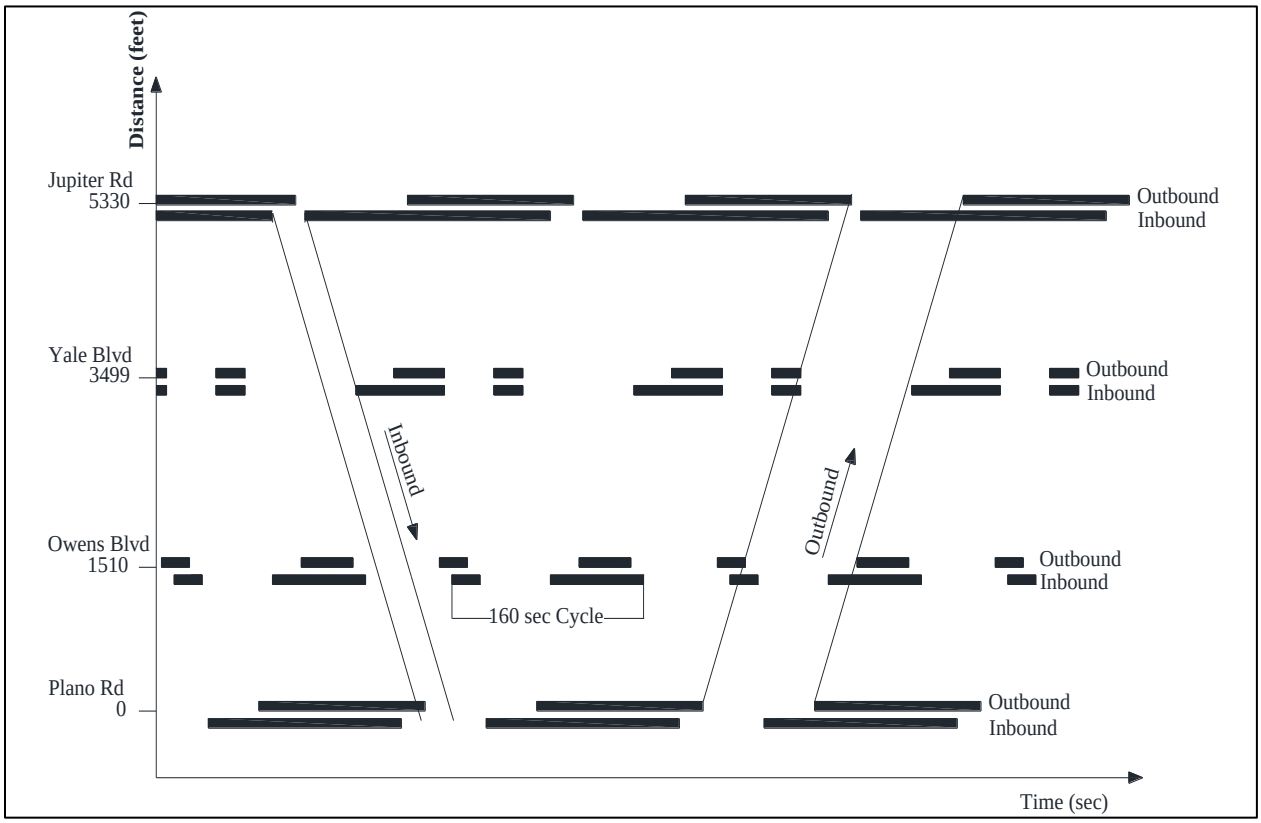

Figure 9. Time-space diagram of case study with UDC scheme

The objective weight is another parameter of interest in this case study. The optimization results are not sensitive to changes in the objective weight (λ^o) when it is greater than 0.03. When the weight changed within a very small range (between 0.0005 and 0.03), the model yielded a smooth Pareto Front. Figure 10 shows the Pareto Front in the case study. It indicates that the UDC control scheme could save at least 4.3 percent of total average delay without reducing bandwidth efficiency very much; and it could save about 4.7 percent of delay at most by sacrificing 40 percent of bandwidth achieved under single cycling. Another trend found with the objective weight analysis is that, as the contribution of delay component to the model objective increased, the difference between the two sub-green splits on arterial decreases in order to minimize delay. The range of objective weight needed to construct a Pareto Front varies depending on the input traffic and geometric data. Usually a larger value of λ^o should be preferred since arterial progression often has higher priority over reducing delay on cross streets.

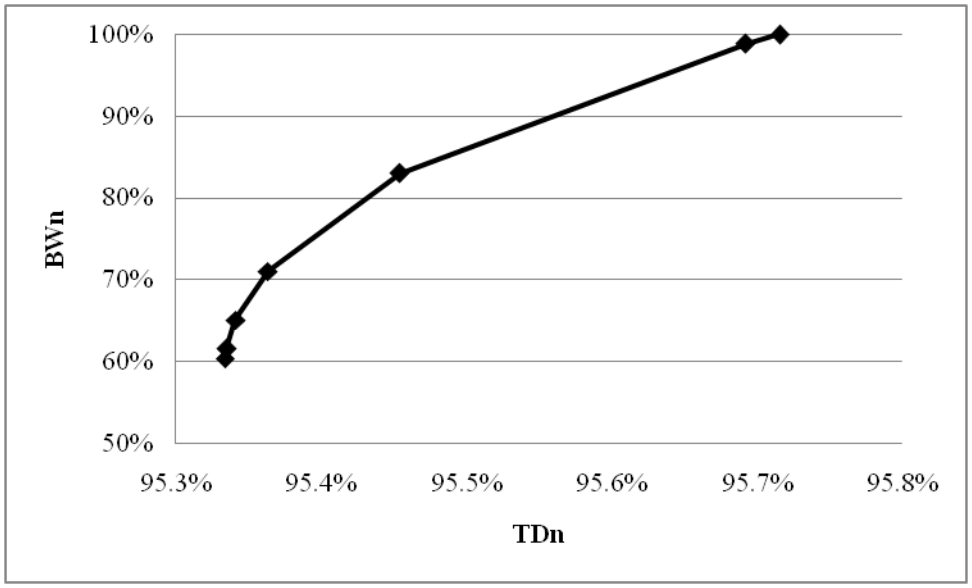

Figure 10. Pareto Front of bandwidth and delay objectives

CHAPTER 4. CONCLUSIONS AND FUTURE STUDY

CONCLUSIONS

Conventional single cycling coordination often causes excessive delay at major-minor intersections when a long background cycle length is dictated by the major-major intersections. With advances in signal controllers, coordination systems need more enhanced timing optimization models to fully exploit their capabilities for efficient design of signal timing.

The proposed model adds flexibility to conventional modeling by using double cycling to reduce total average delay without compromising too much of the bandwidth efficiency. The consideration of delay estimation makes a quadratic objective function, but through disjunctive programming the constraints are all linear, and thus good computational efficiency can be still maintained.

To test and evaluate the developed optimization model, we conducted numerical experiments by varying different input parameters and a case study using field data. Numerical experiments investigated the impacts of several *v/s*-based parameters on the performance of the UDC control scheme. Among the six parameters studied, three of them were chosen as the indicators for checking if double cycling would be beneficial at a major-minor intersection. The results of the numerical experiments are summarized as follows, which could serve as preliminary guidelines for UDC application.

- Bandwidth efficiency does not necessarily change very much with the following three parameters, which are not considered as effective indicators for UDC application.
    - Percentage of left turn *v/s* of the sum of this left turn v/*s* and its opposing through *v/s* on a cross-street approach at the candidate UDC intersection (*CrstLT*)
    - The ratio of critical *v/s* for arterial phases between the candidate UDC intersection and the critical intersection along the arterial (*UtS*)
    - The ratio of volume-to-capacity ratio between the candidate UDC intersection and the critical intersection along the arterial (*Xc-ratio*)
- Bandwidth efficiency generally changes with the following three parameters within a wide range, at least part which is monotone. These parameters are suggested for further developing criteria for UDC application guidance.
    - Percentage of left turn *v/s* of the sum of this left turn v/*s* and its opposing through *v/s* on an arterial approach at the candidate UDC intersection (*ArtLT*)
    - The ratio between the sum of critical *v/s* for arterial phases and the sum of critical *v/s* for cross-street phases at the candidate UDC intersection (*AtC*)
    - The arterial green time ratio between the candidate UDC intersection and the critical intersection under single cycling (*g-ratio*)
- Double cycling generally performs better at intersections with permitted left turn operation.
- Double cycling is not recommended when bandwidth efficiency after adopting the UDC control scheme is reduced by more than 10 percent (*BWn* $\leq$90%).

- Criteria listed in Table 6 might be considered for prechecking if double cycling would be beneficial at a candidate UDC intersection.
- *g-ratio* is suggested as the primary parameter for checking UDC applicability; *AtC* and *ArtLT* are suggested as the auxiliary checking parameters.
- The suggested criteria are results from numerical experiments with limited scenarios, and thus does not necessarily cover all traffic and geometric conditions where double cycling may or may not be beneficial.

Table 6. Preliminary criteria for checking UDC applicability

	***BWn* ≥ 90%**		***BWn* ≥ 95%**		***BWn* ≥ 97%**		***BWn* ≥ 100%**	
	Protected left turn	**Permitted left turn**	**Protected left turn**	**Permitted left turn**	**Protected left turn**	**Permitted left turn**	**Protected left turn**	**Permitted left turn**
***ArtLT* ≤**	0.21	0.21	0.17	0.21	0.15	0.21	NA	0.09
***AtC* ≥**	0.50	0.50	0.55	0.50	0.75	0.50	NA	0.07
***g-ratio* ≥**	1.07	1.15	1.26		1.77		NA	2.06

The case study using field data of a four-intersection arterial followed the guidance developed based on the results of numerical experiments. The prechecking process following the preliminary guidelines suggested UDC be adopted. The actual optimization results showed that the UDC control scheme would achieve the same bandwidth efficiency while saving 4.3 percent of total average vehicular delay as compared with conventional single cycling.

FUTURE STUDY

Limited by the scope of this research, further research is needed to fully understand the advantages and disadvantages of the double cycling optimization. The underlying assumptions and simplifications, i.e., under-saturation, no blockage or spillback, and constant flow conditions, in this model can be relaxed in further study to accommodate more realistic traffic and geometric conditions.

Noting that the above results are based on a small set of test problems, the model needs to test more traffic and geometric scenarios to provide application guidance. For example, the underlying three assumptions do not exclude the scenario when the long background cycle length is required by wide intersections with longer pedestrian timing needs, while volume demands do not necessarily justify a beneficial large cycle length at the double cycled intersections.

The control scheme allocates the slack green time to a sub-cycle to reduce delay at double cycled intersections. This may affect progression quality due to the reduced reliability of letting platoons pass through the double cycled intersection if large traffic variation is presented. Therefore, an interesting research topic would be stochastic analysis of traffic conditions to evaluate progression reliability of the control scheme and provide additional guidance for the application. The optimization model can be revised to also consider stochastic traffic input to generate robust timing plans.

Also, the model could be extended to the network level and provide the option of servicing twice protected left turn if a short turning bay is presented. Another potential research topic is to create secondary green bands to fully make use of different sub-green phases when a large number of intersections is presented in the arterial.

APPENDIX

PARAMETERS

β_i^a (β_i^c) = 0-1 parameter for protected or permitted-only left turn on arterial (cross street) at intersection *i*;

λ^o = weight of the normalized bandwidth objective in the objective function;

$\tau_{i,ja}$ = queue clearance time in advance of the outbound (inbound) bandwidth at intersection *i*, in cycles;

$BW_{\max}$ = weighted sum of two-way bandwidths efficiency under MAXBAND solution;

c = weight of outbound bandwidth efficiency in the bandwidth objective

$d_{i,ja}$ = outbound (inbound) distance between intersection *i* (*i*+1) and intersection *i*+1 (*i*);

$D_{i,j}^L$ = average delay per background cycle for left turn movement *j* at intersection *i*;

$D_{s,j}^{Ts}$ = average delay per background cycle for through movement *j* at single cycled intersection *s*;

$e_{i,ja}$ = lower limit on outbound (inbound) speed on link between intersection *i* (*i*+1) and intersection *i*+1 (*i*);

$f_{i,ja}$ = upper limit on outbound (inbound) speed on link between intersection *i* (*i*+1) and intersection *i*+1 (*i*);

$g_{i,j}^d$ = through green splits on approach *j* at intersection *i* if double cycled, in cycles;

$g_{i,j}^s$ = through green splits on approach *j* at intersection *i* if single cycled, in cycles;

$g_{i,j}^{\min}$ = minimal through green split on approach *j* at intersection *i*,in cycles;

$1/h_{i,ja}$ = lower limit on outbound (inbound) reciprocal speed change between intersection *i* (*i*+1) and intersection *i*+1 (*i*);

k = inbound to outbound target bandwidth ratio;

$l_{i,j}$ =effective left turn split on approach *j* at intersection *i*;

$L_{i,j}$ =effective left turn split plus per-phase lost time on approach *j* at intersection *i*;

N = number of intersections along the arterial;

Nc_i = number of critical phases in a ring under single cycling at intersection *i*;

Ns = number of single cycled intersections along the arterial;

Nu = number of double cycled intersections along the arterial;

$1/o_{i,ja}$ = lower limit on outbound (inbound) reciprocal change between intersection *i* (*i*+1) and intersection *i*+1 (*i*);

$TD_{\max}$ = total average uniform delay under single cycling;

$y_{i,cj}$ = v/s ratio of critical phase *cj* on at intersection *i*;

$y_{i,j}^L$ = v/s ratio for left turn movement on approach *j* at intersection *i*;

$y_{i,j}^T$ = v/s ratio for through movement on approach *j* at intersection *i*;

Y = per phase lost time, in cycles;

z = inverse of background cycle length.

DECISION VARIABLES

$\alpha_{u,j}^{I1}$ = 0-1 variable for replacing the absolute function for approach *j* at double cycled intersection *u*, $\alpha_{u,j}^{I1} = | \theta_{u,j} - \delta_{u,j} |$;

$\alpha_{u,ja}^{I2}$ = 0-1 variable for replacing the product function for approach *ja* at double cycled intersection *u*, $\alpha_{u,ja}^{I2} = \theta_{u,ja}\delta_{u,ja}$;

$\delta_{i,j}$ = 0-1 decision variable for lagging (1) or leading (0) left turn pattern on approach *j* at intersection *i*;

Δ_i = time from the center of $r_{i,2}^N$ to the nearest center of $r_{i,1}^N$; positive if the center of $r_{i,1}^N$ is to the right of the center of $r_{i,2}^N$, in cycles;

$\lambda_{u,j}^{D1}$ = 0-1 variable for disjunctive constraint related to $\alpha_{u,j}^{I1}$ for approach *j* at double cycled intersection *u;*

$\lambda_{u,j}^{D2}$ = 0-1 variable for disjunctive constraint related to $t1_{u,j}$ for approach *j* at double cycled intersection *u;*

$\lambda_{u,ja}^{D3}$ = 0-1 variable for disjunctive constraint related to $\alpha_{u,ja}^{I2}$ for approach *ja* at double cycled intersection *u;*

λ_{u}^{D4} = 0-1 variable for disjunctive constraint related to selecting sub-green for band passage at double cycled intersection *u;*

$\theta_{u,j}$ = 0-1 variable for selecting the first sub-cycle for protected left turn phase on approach *j* at double cycled intersection *u*, in cycles;

b_{ja} = outbound (inbound) bandwidth efficiency, in cycles;

$g1_{u,j}$ = sub-green split in the first sub-cycle for through movement on approach *j* at double cycled intersection *u*, in cycles;

$g2_{u,j}$ = sub-green split in the second sub-cycle for through movement on approach *j* at double cycled

m_i = an integer number;

$r1_{u,j}$ = sub-red split in the first sub-cycle for through movement on approach *j* at double cycled intersection *u*, in cycles;

$r2_{u,j}$ = sub-red split in the second sub-cycle for through movement on approach *j* at double cycled intersection *u*, in cycles;

$r_{i,ja}^N$ = arterial nominal red split on approach *ja* at intersection *i*, in cycles;

$t_{i,ja}$ = arterial outbound (inbound) travel time from intersection *i* (*i*+1) to intersection *i*+1 (*i*), in cycles;

$t1_{u,j}$ = actual through queue discharge time in the first sub-cycle on approach *j* at double cycled intersection *u*, in cycles;

$w_{i,ja}$ = time from right (left) side of red at intersection *i* to left (right) edge of outbound (inbound) green band, in cycles;

INTERIM VARIABLES

BW = weighted sum of two-way bandwidths efficiency under double cycling before normalization;

BW_{nor} = normalized bandwidths efficiency for double cycling;

$D_{u,j}^{Td}$ = average delay per background cycle for through movement *j* at double cycled intersection *u*;

$R1_{u,ja}$ = total phase splits in the first sub-cycle on approach ja at double cycled intersection *u*, in cycles;

$R2_{u,ja}$ = total phase splits in the second sub-cycle on approach ja at double cycled intersection *u*, in cycles;

TD = weighted total average uniform delay under double cycling before normalization;

TD_{nor} = normalized total average uniform delay for double cycling;

INDICES

i = intersection ID, $i = 1, 2, 3...N$;

j = approach ID, $j = 1, 2...4$;

ja = arterial approach ID, 1 for outbound, 2 for inbound;

jc = cross street approach ID, 3 for outbound, 4 for inbound;

s = single cycled intersection ID, $s = 1, 2, 3...Ns$

u = double-cycled intersection ID, $u = 1, 2, 3...Nu$

REFERENCES

1. Kurfees, W., Using Uneven Double Cycles to Improve the Effectiveness of Arterial Traffic Signal Operations, Managing Congestion--Can We Do Better? Institute of Traffic Engineer (ITE) 2007 Technical Conference and Exhibit, San Diego CA, March, 2007.
2. Synchro Studio 7 User Guide, Trafficware, Sugar Land, TX, USA, 2006.
3. Morgan, J. T. and Little, J. D. C., "Synchronizing Traffic Signals for Maximal Bandwidth," *Operations. Research*, vol. 12, NO. 6, pp. 896–912, December 1964.
4. Chaudhary, N. A., Pinnoi, A., and Messer, C. J. Proposed Enhancements to MAXBAND 86 Program. *Transportation Research Record: Journal of the Transportation Research Board, No. 1324*, Transportation Research Board of the National Academies, Washington, D.C., 1991, pp. 98-104.
5. Gartner, N. H.; Assman, S. F.; Lasaga, F.; Hou, D. L. A Multi-Band Approach to Arterial Traffic Signal Optimization, *Transportation Research Part B: Methodological*, 25 (1), Transportation Research Board of the National Academies, Washington, D.C., 1991, pp. 55-74.
6. Tian, Z. and Urbanik, T., "System partition technique to improve signal coordination and traffic progression," *Journal of Transportation Engineering, ASCE*, vol. 133, NO. 2, pp. 119–128, January. 2007.
7. Chaudhary, N. A.; Pinnoi, A.; Messer, C. J., Scheme to Optimize Circular Phasing Sequences, *Transportation Research Record, Journal of the Transportation Research Board, No. 1324*, Transportation Research Board of the National Academies, Washington, D.C., 1991, pp. 72-82.
8. Mc Trans, *Traffic Network Study Tool, Transyt-7F, United States Version*, May 11, 2011, http://mctrans.ce.ufl.edu/featured/transyt-7f/, accessed November 11, 2012.
9. Cohen, S. L., Concurrent Use of MAXBAND and TRANSYT Signal Timing Programs for Arterial Signal Optimization. *Transportation Research Record, Journal of the Transportation Research Board, No. 906*, Transportation Research Board of the National Academies, Washington, D.C., 1983, pp. 81-84.
10. Skabardonis, A. and May, A. D., Comparative Analysis of Computer Models for Arterial Signal Timing, *Transportation Research Record Journal of the Transportation Research Board, No. 1021*, 1985, pp. 45–52.
11. Liu, C. C., Bandwidth-Constrained Delay Optimization for Signal Systems, *Institute of Traffic Engineer (ITE) Journal*, 58 (12), pp. 21-26, 1988.
12. Lan, C. J. and Messer, C. J., Compromise Approach to Optimize Traffic Signal Coordination Problems during Unsaturated conditions, Transportation Research Record, Journal of the Transportation Research Board, No. 1360, Transportation Research Board of the National Academies, Washington, D.C., 1992, pp. 112-120.
13. Transportation Research Board, *Highway Capacity Manual, 5th Edition (HCM 2010)*, Transportation Research Board of the National Academies, 2010.
14. IBM, *IBM ILOG CPLEX Optimization Studio V12.6.0 documentation*, October 1, 2013, http://pic.dhe.ibm.com/infocenter/cosinfoc/v12r6/index.jsp, accessed November 10, 2013.